

## Two-Wire True Zero Speed Miniature Differential Peak-Detecting Gear Tooth Sensor with Continuous Calibration

---

### Not for New Design

These parts are in production but have been determined to be NOT FOR NEW DESIGN. This classification indicates that sale of this device is currently restricted to existing customer applications. The device should not be purchased for new design applications because obsolescence in the near future is probable. Samples are no longer available.

Date of status change: October 1, 2022

#### Recommended Substitutions:

*For existing customer transition, and for new customers or new applications, refer to the [ATS19200LSNATN-L](#) or [ATS19200LSNATN-H](#).*

---

NOTE: For detailed information on purchasing options, contact your local Allegro field applications engineer or sales representative.

---

*Allegro MicroSystems reserves the right to make, from time to time, revisions to the anticipated product life cycle plan for a product to accommodate changes in production capabilities, alternative product availabilities, or market demand. The information included herein is believed to be accurate and reliable. However, Allegro MicroSystems assumes no responsibility for its use; nor for any infringements of patents or other rights of third parties which may result from its use.*

---

## Two-Wire True Zero Speed Miniature Differential Peak-Detecting Gear Tooth Sensor with Continuous Calibration

### Features and Benefits

- Running mode calibration for continuous optimization
- Single chip IC for high reliability
- Internal current regulator for 2-wire operation
- Small mechanical size (8 mm diameter × 5.5 mm depth)
- Precise duty cycle signal over operating temperature range
- Large operating air gaps
- Automatic Gain Control (AGC) for air gap independent switchpoints
- Automatic Offset Adjustment (AOA) for signal processing optimization
- True zero-speed operation
- Undervoltage lockout
- Wide operating voltage range

### Package: 4-pin Module (suffix SH)



Not to scale

### Description

The ATS642LSH is an optimized Hall effect sensing integrated circuit and magnet combination that provides a user-friendly solution for true zero-speed digital gear-tooth sensing in two-wire applications. The sensor consists of a single-shot molded plastic package that includes a samarium cobalt magnet, a pole piece, and a Hall effect IC that has been optimized to the magnetic circuit. This small package, with optimized two-wire leadframe, can be easily assembled and used in conjunction with a wide variety of gear shapes and sizes.

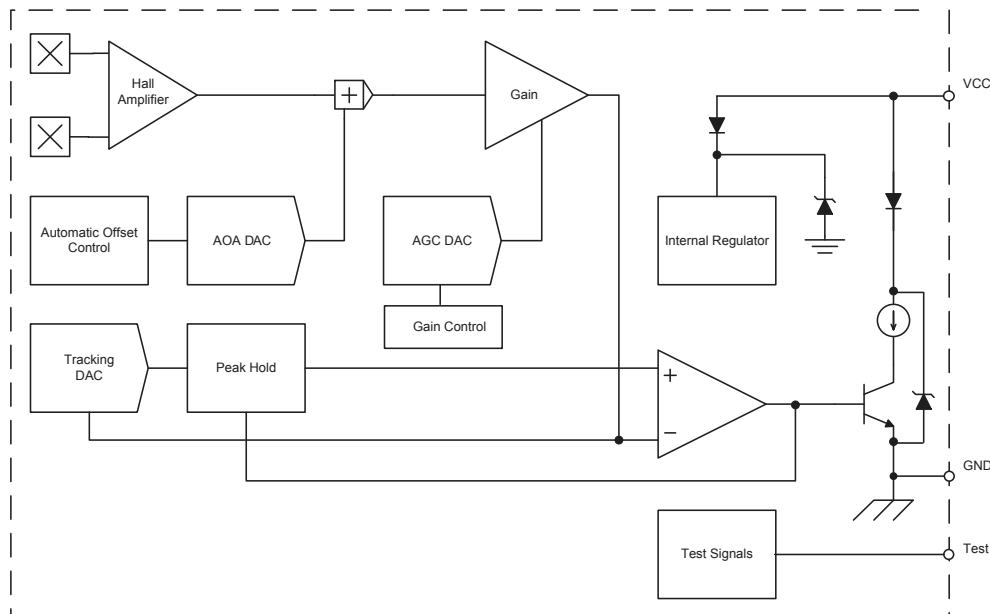
The integrated circuit incorporates a dual element Hall effect sensor and signal processing that switches in response to differential magnetic signals created by ferrous gear teeth. The circuitry contains a sophisticated digital circuit to reduce magnet and system offsets, to calibrate the gain for air gap independent switchpoints, and to achieve true zero-speed operation. Signal optimization occurs at power-up through the combination of offset and gain adjust and is maintained throughout the operating time with the use of a running mode calibration. The running mode calibration allows immunity to environmental effects such as microoscillations of the target or sudden air gap changes.

The regulated current output is configured for two wire applications and the sensor is ideally suited for obtain-

*Continued on the next page...*

Engineering samples available on a limited basis. Contact your local sales or applications support office for additional information.

### Functional Block Diagram



# ATS642LSH

## Two-Wire True Zero Speed Miniature Differential Peak-Detecting Gear Tooth Sensor with Continuous Calibration

### Description (continued)

ing speed and duty cycle information in ABS (antilock braking systems). The 1.5 mm Hall element spacing is optimized for fine pitch gear-tooth-based configurations. The package is lead (Pb) free, with 100% matte tin leadframe plating.

### Selection Guide

Part Number	I <sub>CC</sub> Typical	Packing*
ATS642LSHTN-I1-T	6.0 Low to 14.0 High mA	Tape and reel, 13-inch reel 800 pieces/reel
ATS642LSHTN-I2-T	7.0 Low to 14.0 High mA	

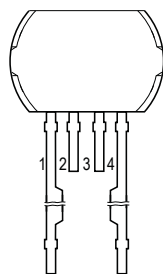


\*Contact Allegro™ for additional packing options

### Absolute Maximum Ratings

Characteristic	Symbol	Notes	Rating	Unit
Supply Voltage	V <sub>CC</sub>		28	V
Reverse_Supply Voltage	V <sub>RCC</sub>		-18	V
Operating Ambient Temperature	T <sub>A</sub>	Range L	-40 to 150	°C
Maximum Junction Temperature	T <sub>J(max)</sub>		165	°C
Storage Temperature	T <sub>stg</sub>		-65 to 170	°C

### Pin-out Diagram



### Terminal List

Number	Name	Function
1	VCC	Connects power supply to chip
2	NC	No connection
3	Test pin	Float or tie to GND
4	GND	Ground terminal

**OPERATING CHARACTERISTICS** using reference target 60-0,  $T_A$  and  $V_{CC}$  within specification, unless otherwise noted

Characteristic	Symbol	Test Conditions	Min.	Typ. <sup>1</sup>	Max.	Units
<b>ELECTRICAL CHARACTERISTICS</b>						
Supply Voltage <sup>2</sup>	$V_{CC}$	Operating; $T_J < 165\text{ }^\circ\text{C}$	4.0	–	24	V
Undervoltage Lockout	$V_{CC(UV)}$	$V_{CC} 0 \rightarrow 5\text{ V}$ and $5 \rightarrow 0\text{ V}$	–	–	4.0	V
Supply Zener Clamp Voltage	$V_Z$	$I_{CC} = I_{CC(max)} + 3\text{ mA}$ ; $T_A = 25\text{ }^\circ\text{C}$	28	–	–	V
Supply Zener Current	$I_Z$	Test conditions only; $V_Z = 28\text{ V}$	–	–	$I_{CC(max)}^+ 3\text{ mA}$	mA
Supply Current	$I_{CC(Low)}$	ATS642LSH-I1	4.0	6.0	8.0	mA
		ATS642LSH-I2	5.9	7.0	8.4	mA
	$I_{CC(High)}$	ATS642LSH-I1	12.0	14.0	16.0	mA
		ATS642LSH-I2	11.8	14.0	16.8	mA
Supply Current Ratio	$I_{CC(High)}/I_{CC(Low)}$	Ratio of high current to low current	1.85	–	3.05	–
Reverse Battery Current	$I_{RCC}$	$V_{RCC} = -18\text{ V}$	–	–	-5	mA
<b>POWER-ON STATE CHARACTERISTICS</b>						
Power-On State <sup>3</sup>	POS	$t > t_{PO}$	–	$I_{CC(High)}$	–	–
Power-On Time <sup>4</sup>	$t_{PO}$	Target gear speed $< 100\text{ rpm}$	–	1	2	ms
<b>OUTPUT STAGE</b>						
Output Slew Rate <sup>5</sup>	$dl/dt$	$R_{LOAD} = 100\ \Omega$ , $C_{LOAD} = 10\text{ pF}$	–	10	–	mA/ $\mu\text{s}$

Continued on the next page.

# ATS642LSH

## Two-Wire True Zero Speed Miniature Differential Peak-Detecting Gear Tooth Sensor with Continuous Calibration

**OPERATING CHARACTERISTICS** (continued) using reference target 60-0,  $T_A$  and  $V_{CC}$  within specification, unless otherwise noted

Characteristic	Symbol	Test Conditions	Min.	Typ. <sup>1</sup>	Max.	Units
<b>SWITCHPOINT CHARACTERISTICS</b>						
Rotation Speed	$S_{ROT}$	Reference Target 60-0	0	–	8,000	rpm
Analog Signal Bandwidth	BW	Equivalent to $f - 3$ dB	20	40	–	kHz
Operate Point	$B_{OP}$	Transitioning from $I_{CC(High)}$ to $I_{CC(Low)}$ ; positive peak referenced; $AG < AG_{MAX}$	–	120	–	mV
Release Point	$B_{RP}$	Transitioning from $I_{CC(Low)}$ to $I_{CC(High)}$ ; negative peak referenced; $AG < AG_{MAX}$	–	120	–	mV
<b>CALIBRATION</b>						
Initial Calibration	$C_1$	Quantity of rising output (current) edges required for accurate edge detection	–	–	3	Edge
<b>DAC CHARACTERISTICS</b>						
Allowable User-Induced Differential Offset		Output switching only; may not meet datasheet specifications	–	$\pm 60$	–	G
<b>FUNCTIONAL CHARACTERISTICS<sup>6</sup></b>						
Operational Air Gap Range <sup>7</sup>	AG	$\Delta DC$ within specification	0.5	–	2.75	mm
Maximum Operational Air Gap Range	$AG_{OP(max)}$	Output switching (no missed edges); $\Delta DC$ not guaranteed	–	–	3	mm
Duty Cycle Variation	$\Delta DC$	Wobble $< 0.5$ mm; Typical value at $AG = 1.5$ mm, for max., min., AG within specification	41	–	61	%
Duty Cycle Pitch Variance <sup>8</sup>	$E_{DC}$	$AG = 1.5$ mm	–	$\pm 1.5$	–	%
Operating Signal Range <sup>9</sup>	Sig	Operating within specification	30	–	1000	G
Minimum Operating Signal	$Sig_{OP(min)}$	Output switching (no missed edges); $\Delta DC$ not guaranteed	20	–	–	G

<sup>1</sup>Typical values are at  $T_A = 25^\circ C$  and  $V_{CC} = 12$  V. Performance may vary for individual units, within the specified maximum and minimum limits.

<sup>2</sup>Maximum voltage must be adjusted for power dissipation and junction temperature; see *Power Derating* section.

<sup>3</sup>Please refer to Sensor Operation section, page 13.

<sup>4</sup>Power-On Time includes the time required to complete the internal automatic offset adjust. The DACs are then ready for peak acquisition.

<sup>5</sup>dl is the difference between 10% of  $I_{CC(Low)}$  and 90% of  $I_{CC(High)}$ , and dt is time period between those two points.

Note:  $di/dt$  is dependent upon the value of the bypass capacitor, if one is used.

<sup>6</sup>Functional characteristics valid only if magnetic offset is within the specified range for Allowable User Induced Differential Offset.

<sup>7</sup>AG is dependent on the available magnetic field. The available field is dependent on target geometry and material, and should be independently characterized. The field available from the reference target is given in the reference target parameter section of the datasheet.

<sup>8</sup> $E_{DC}$  represents the difference between consecutive duty cycles,  $DC(n) - DC(n-1)$ ; Mean  $\pm 3$ -sigma.

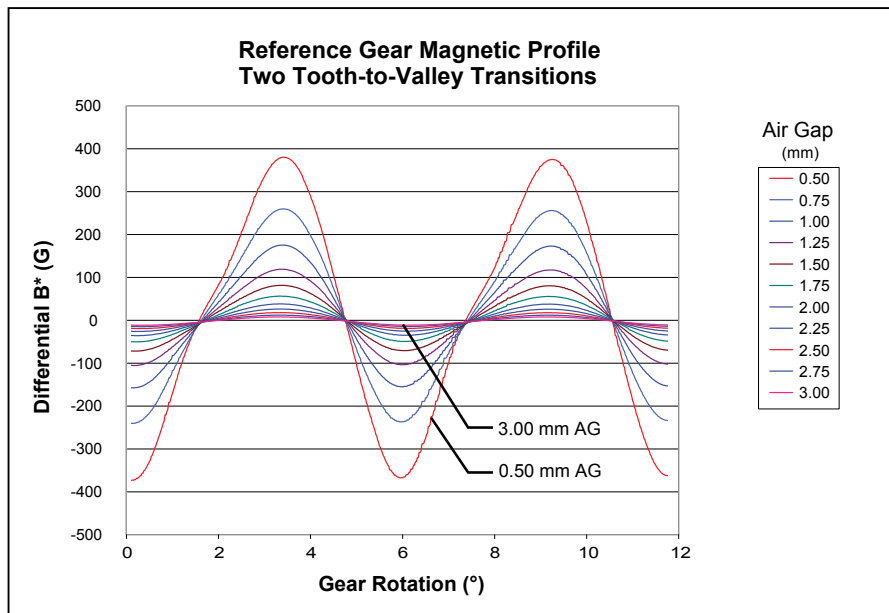
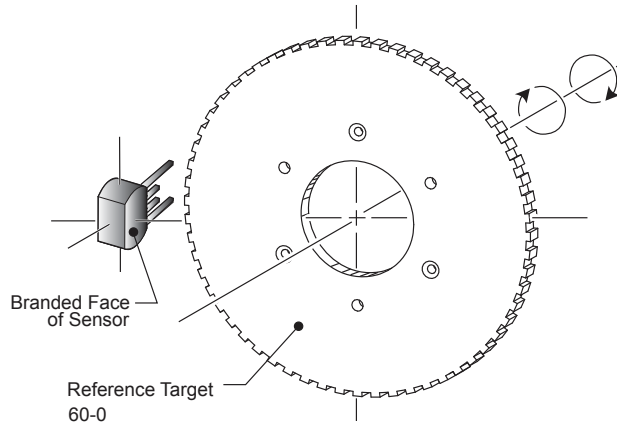
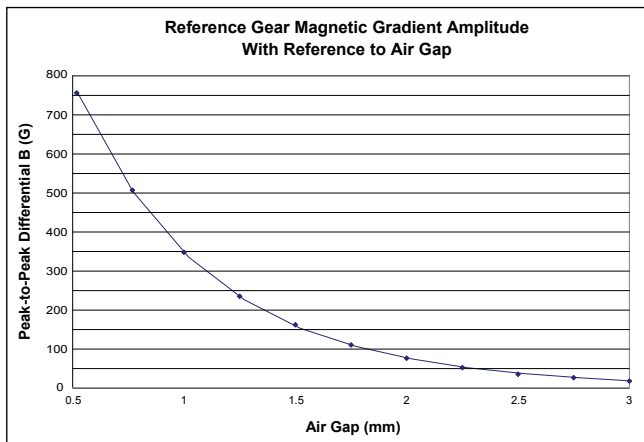
<sup>9</sup>In order to remain in specification, the magnetic gradient must induce an operating signal greater than the minimum value specified. This includes the effect of target wobble.

# ATS642LSH

## Two-Wire True Zero Speed Miniature Differential Peak-Detecting Gear Tooth Sensor with Continuous Calibration

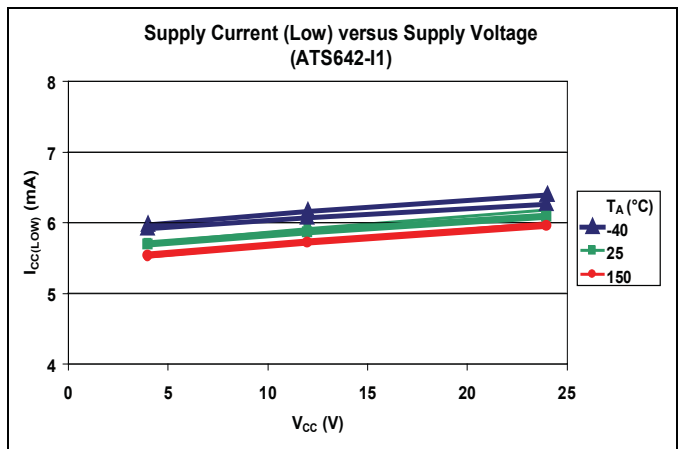
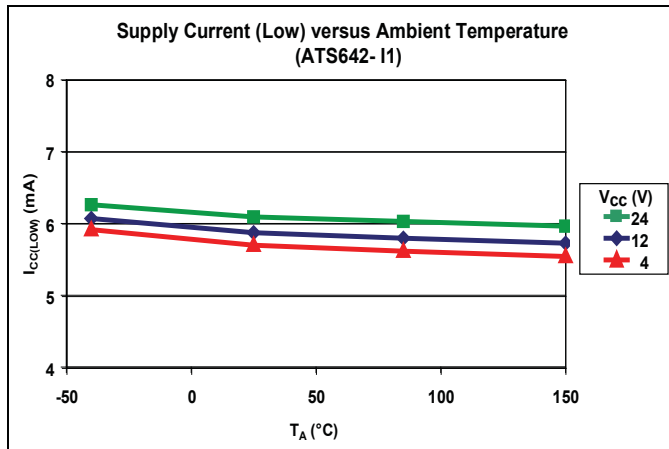
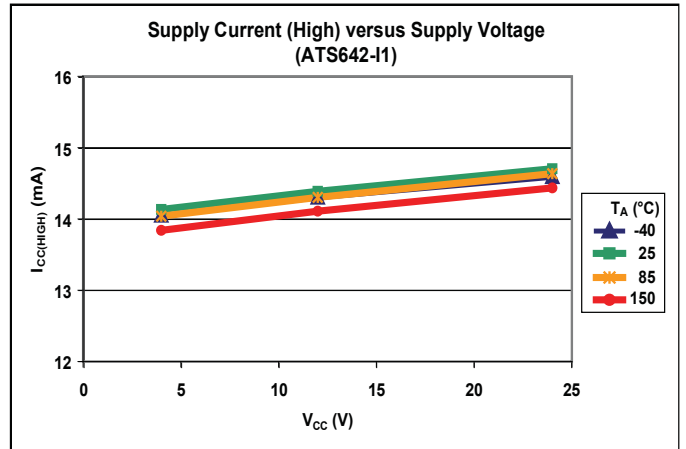
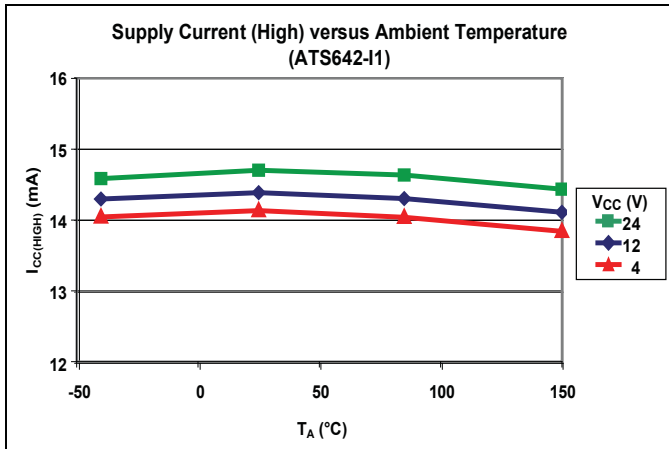
### REFERENCE TARGET, 60-0 (60 Tooth Target)

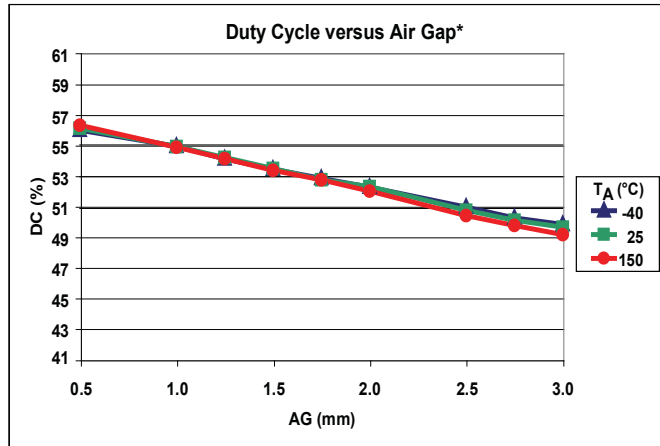
Characteristics	Symbol	Test Conditions	Typ.	Units	Symbol Key
Outside Diameter	$D_o$	Outside diameter of target	120	mm	
Face Width	F	Breadth of tooth, with respect to sensor	6	mm	
Angular Tooth Thickness	t	Length of tooth, with respect to sensor	3	deg	
Angular Valley Thickness	$t_v$	Length of valley, with respect to sensor	3	deg	
Tooth Whole Depth	$h_t$		3	mm	
Material		Low Carbon Steel	-	-	



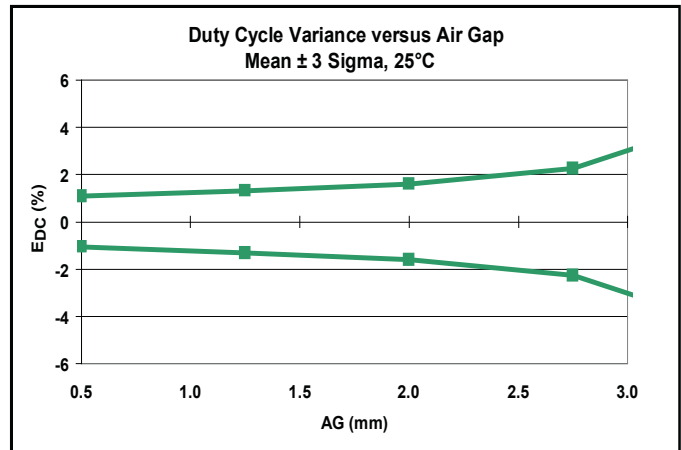
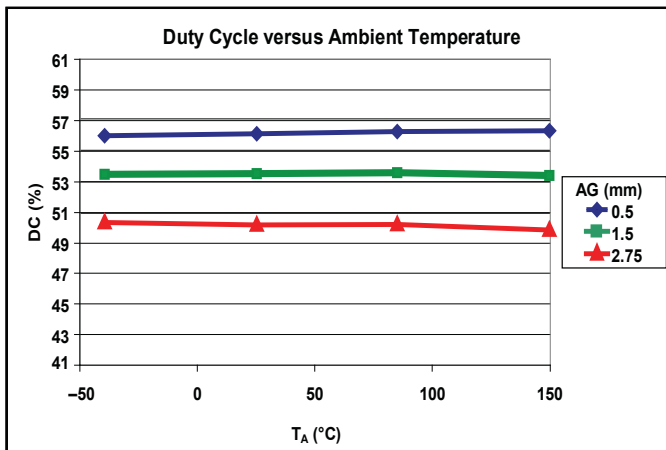
### Characteristic Data

I1 Trim



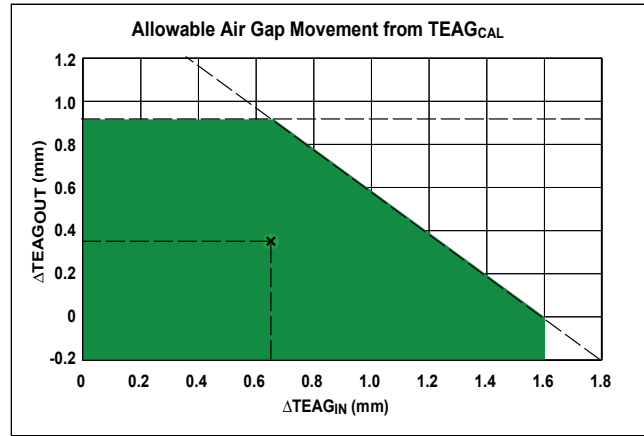


\*The trend of duty cycle versus air gap is driven by the actual magnetic profile of the target (see figure on page 5).



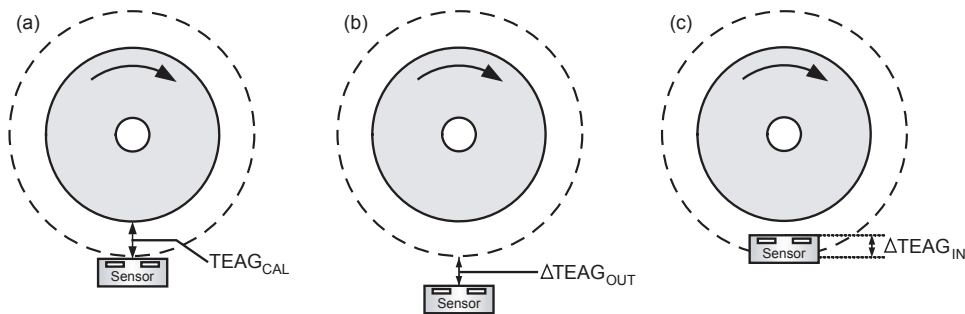


### Characteristic Allowable Air Gap Movement 60-0 (60 Tooth Target)



The colored area in the chart above shows the region of allowable air gap movement within which the sensor will continue output switching. The output duty cycle is wholly dependent on the target's magnetic signature across the air gap range of movement, and may not always be within specification throughout the entire operating region (to  $AG_{OPmax}$ ).

The axis parameters for the chart are defined in the drawings below. As an example, assume the case where the air gap is allowed to vary from from the nominal installed air gap ( $TEAG_{CAL}$ , panel a) within the range defined by an increase of  $\Delta TEAG_{OUT} = 0.35$  mm (shown in panel b), and a decrease of  $\Delta TEAG_{IN} = 0.65$  mm (shown in panel c). This case is plotted with an "x" in the chart above.



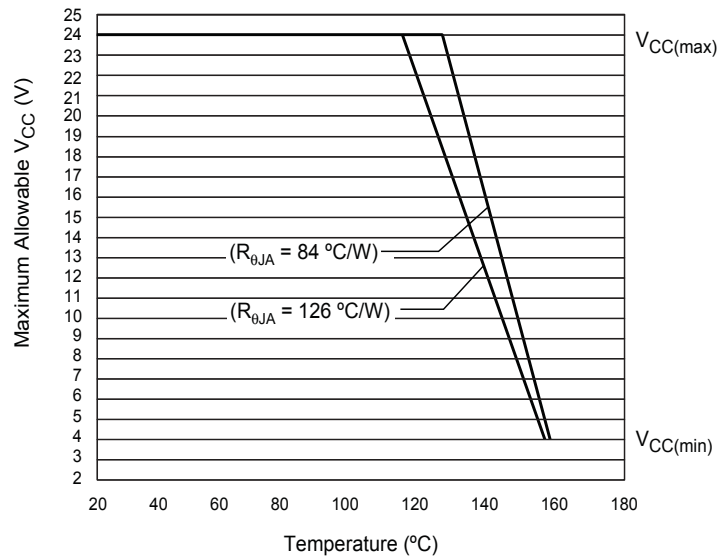
For more information on these figures and the calculations used to generate them, please refer to the Applications Note *Determining Allowable Air Gap Variation for the ATS642*.

**THERMAL CHARACTERISTICS** may require derating at maximum conditions, see application information

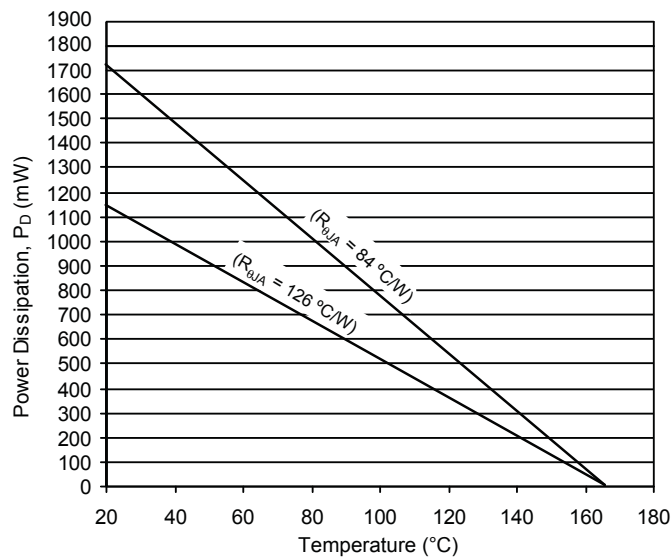
Characteristic	Symbol	Test Conditions*	Value	Units
Package Thermal Resistance	$R_{\theta JA}$	Single-layer PCB with copper limited to solder pads	126	$^{\circ}\text{C}/\text{W}$
		Two-layer PCB with 3.8 in. <sup>2</sup> of copper area on each side connected with thermal vias and to device ground pin	84	$^{\circ}\text{C}/\text{W}$

\*Additional information is available on the Allegro Web site.

Power Derating Curve



Maximum Power Dissipation,  $P_{D(\text{max})}$



## Functional Description

### Sensing Technology

The gear tooth sensor subassembly contains a single-chip differential Hall effect sensor IC, an optimized samarium cobalt magnet, and a flat ferrous pole piece. The Hall IC possesses two Hall elements, which sense the magnetic profile of the ferrous target simultaneously, but at different points (spaced at a 1.5 mm pitch), generating a differential internal analog voltage ( $V_{PROC}$ ) that is processed for precise switching of the digital output signal.

The Hall IC is self-calibrating and also possesses a temperature compensated amplifier and offset compensation circuitry. Its voltage regulator provides supply noise rejection throughout the operating voltage range. Changes in temperature do not greatly affect this device due to the stable amplifier design and the offset compensation circuitry. The Hall transducers and signal processing electronics are integrated on the same silicon substrate, using a proprietary BiCMOS process.

### Target Profiling

An operating device is capable of providing digital information that is representative of the mechanical features on a rotating target. The waveform diagram shown in figure 3 presents the automatic translation of the mechanical profile, through the magnetic profile that it induces, to the digital output signal of the sensor.

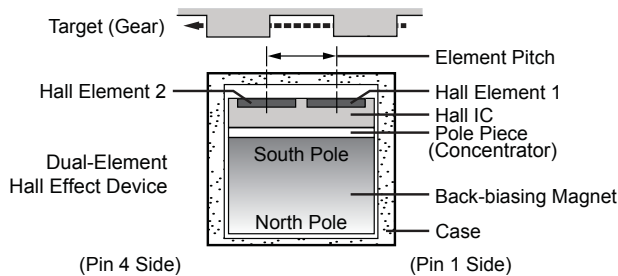


Figure 1. Relative motion of the target is detected by the dual Hall elements mounted on the Hall IC.

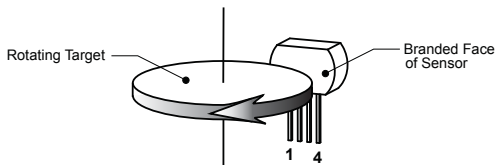


Figure 2. This left-to-right (pin 1 to pin 4) direction of target rotation results in a low output signal when a tooth of the target gear is nearest the face of the sensor (see figure 3). A right-to-left (pin 4 to pin 1) rotation inverts the output signal polarity.

### Output Polarity

Figure 3 shows the output polarity for the orientation of target and sensor shown in figure 2. The target direction of rotation shown is: perpendicular to the leads, across the face of the device, from the pin 1 side to the pin 4 side. This results in the sensor output switching from high,  $I_{CC(High)}$ , to low  $I_{CC(Low)}$ , as the leading edge of a tooth (a rising mechanical edge, as detected by the sensor) passes the sensor face. In this configuration, the device output current switches to its low polarity when a tooth is the target feature nearest to the sensor. If the direction of rotation is reversed, then the output polarity inverts.

Note that output voltage polarity is dependent on the position of the sense resistor,  $R_{SENSE}$  (see figure 4).

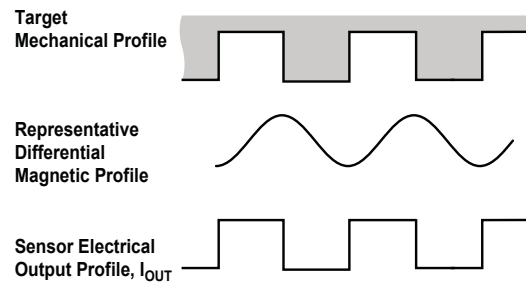


Figure 3. Output Profile of a ferrous target for the polarity indicated in figure 2.

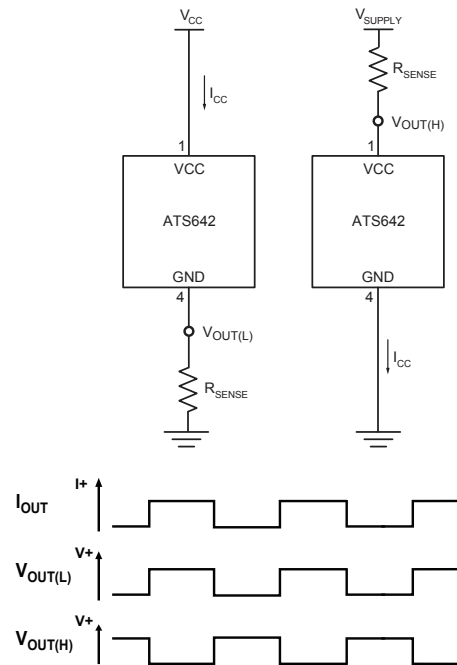


Figure 4: Voltages profiles for high side and low side two-wire sensing.

### Automatic Gain Control (AGC)

This feature allows the device to operate with an optimal internal electrical signal, regardless of the air gap (within the AG specification). During calibration, the device determines the peak-to-peak amplitude of the signal generated by the target. The gain of the sensor is then automatically adjusted. Figure 5 illustrates the effect of this feature.

### Automatic Offset Adjust (AOA)

The AOA is patented circuitry that automatically compensates for the effects of chip, magnet, and installation offsets. (For capability, see Dynamic Offset Cancellation, in the Operating Characteristics table.) This circuitry is continuously active, including both during calibration mode and running mode, compensating for any offset drift. Continuous operation also allows it

to compensate for offsets induced by temperature variations over time.

### Digital Peak Detection

A digital DAC tracks the internal analog voltage signal  $V_{PROC}$ , and is used for holding the peak value of the internal analog signal. In the example shown in figure 6, the DAC would first track up with the signal and hold the upper peak's value. When  $V_{PROC}$  drops below this peak value by  $B_{OP}$ , the device hysteresis, the output would switch and the DAC would begin tracking the signal downward toward the negative  $V_{PROC}$  peak. Once the DAC acquires the negative peak, the output will again switch states when  $V_{PROC}$  is greater than the peak by the value  $B_{RP}$ . At this point, the DAC tracks up again and the cycle repeats. The digital tracking of the differential analog signal allows the sensor to achieve true zero-speed operation.

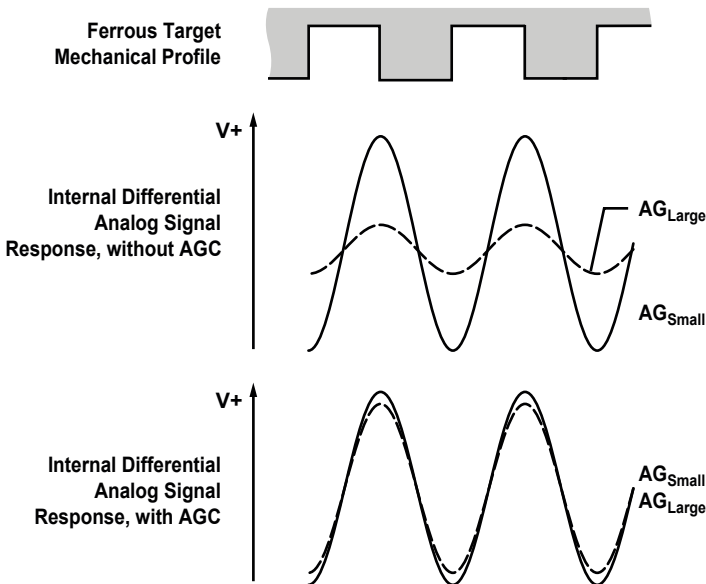


Figure 5. Automatic Gain Control (AGC). The AGC function corrects for variances in the air gap. Differences in the air gap affect the magnetic gradient, but AGC prevents that from affecting device performance, as shown in the lowest panel.

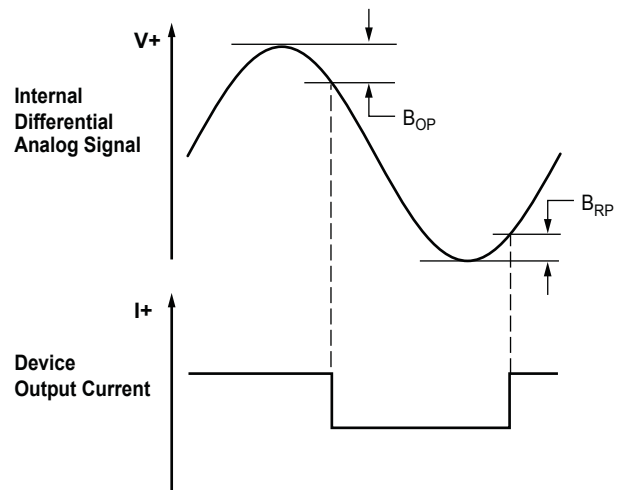


Figure 6: Peak Detecting Switchpoint Detail

### Power Supply Protection

The device contains an on-chip regulator and can operate over a wide  $V_{CC}$  range. For devices that need to operate from an unregulated power supply, transient protection must be added externally. For applications using a regulated line, EMI/RFI protection may still be required. Contact Allegro Microsystems for information on the circuitry needed for compliance with various EMC specifications. Refer to figure 7 for an example of a basic application circuit.

### Undervoltage Lockout

When the supply voltage falls below the undervoltage lockout voltage,  $V_{CC(UV)}$ , the device enters Reset, where the output state returns to the Power-On State (POS) until sufficient  $V_{CC}$  is supplied.  $I_{CC}$  levels may not meet datasheet limits when  $V_{CC} < V_{CC(min)}$ .

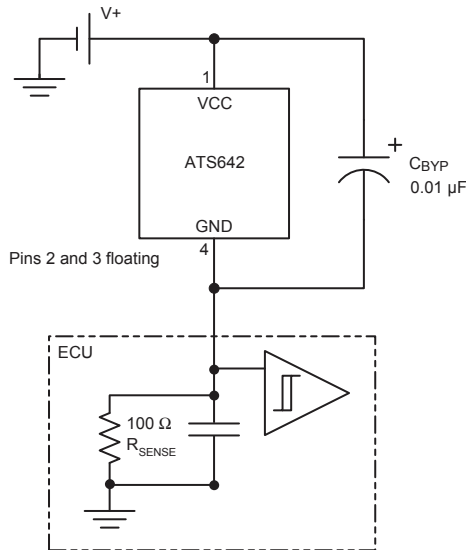


Figure 7: Typical Application Circuit

### Assembly Description

This sensor is integrally molded into a plastic body that has been optimized for size, ease of assembly, and manufacturability. High operating temperature materials are used in all aspects of construction.

### Diagnostics

The regulated current output is configured for two-wire applications, requiring one less wire for operation than do switches with the more traditional open-collector output. Additionally, the system designer inherently gains diagnostics because there is always output current flowing, which should be in either of two narrow ranges, shown in figure 8 as  $I_{CC(High)}$  and  $I_{CC(Low)}$ . Any current level not within these ranges indicates a fault condition. If  $I_{CC} > I_{CC(High)max}$ , then a short condition exists, and if  $I_{CC} < I_{CC(Low)min}$ , then an open condition exists. Any value of  $I_{CC}$  between the allowed ranges for  $I_{CC(High)}$  and  $I_{CC(Low)}$  indicates a general fault condition.

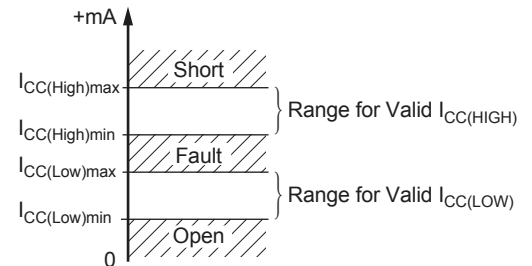


Figure 8: Diagnostic Characteristics of Supply Current Values

### Sensor Operation

Each operating mode is described in detail below.

#### Power-On

When power ( $V_{CC} > V_{CCMIN}$ ) is applied to the device, a short period of time is required to power the various portions of the IC. During this period, the ATS642 will power-on in the high current state,  $I_{CC(High)}$ . After power on, there are conditions that could induce a change in the output state. Such an event could be caused by thermal transients, but would require a static applied magnetic field, proper signal polarity, and particular direction and magnitude of internal signal drift.

#### Initial Offset Adjust

The sensor initially cancels the effects of chip, magnet, and installation offsets. Once offsets have been cancelled, the digital tracking DAC is ready to track the signal and provide output switching. The period of time required for both Power-On and Initial Offset Adjust is defined as the Power-On Time.

#### Calibration Mode

The calibration mode allows the sensor to automatically select the proper signal gain and continue to adjust for offsets. The

AGC is active, and selects the optimal signal gain based on the amplitude of the  $V_{PROC}$  signal. Following each adjustment to the AGC DAC, the Offset DAC is also adjusted to ensure the internal analog signal is properly centered.

During this mode, the tracking DAC is active and output switching occurs, but the duty cycle is not guaranteed to be within specification.

#### Running Mode

After the Initial Calibration period,  $C_1$ , establishes a signal gain, the device moves to Running mode. During Running mode, the sensor tracks the input signal and gives an output edge for every peak of the signal. AOA remains active to compensate for any offset drift over time.

The ATS642 incorporates a novel algorithm for adjusting the signal gain during Running mode. This algorithm is designed to optimize the  $V_{PROC}$  signal amplitude in instances where the magnetic signal “seen” during the calibration period is not representative of the amplitude of the magnetic signal for the installed sensor air gap (see figure 9).

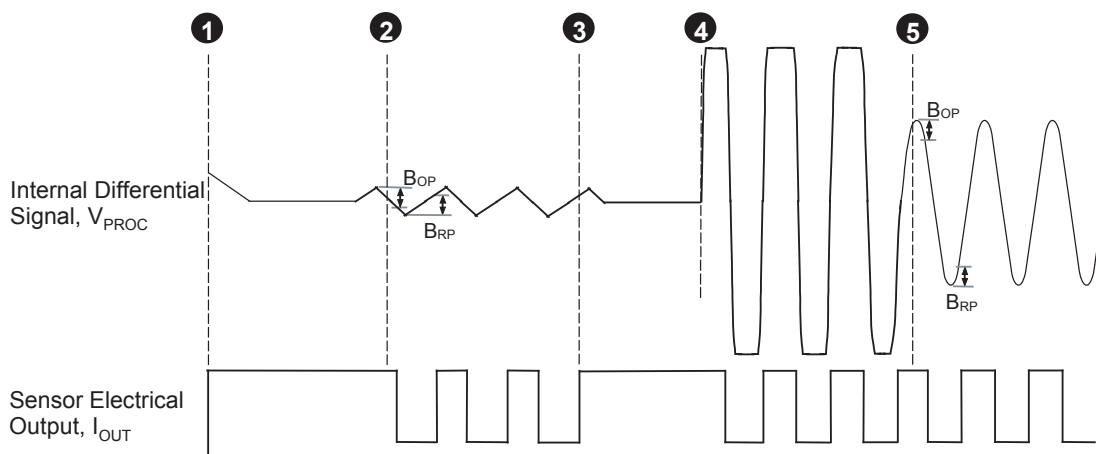


Figure 9: Operation of Running Mode Gain Adjust.

Position 1. The device is initially powered-on. Self-calibration occurs.

Position 2. Small amplitude oscillation of the target sends an erroneously small differential signal to the sensor. The amplitude of  $V_{PROC}$  is greater than the switching hysteresis ( $B_{OP}$  and  $B_{RP}$ ), and the device output switches.

Position 3. The calibration period completes on the third rising output edge, and the device enters Running mode.

Position 4. True target rotation occurs and the correct magnetic signal is generated for the installation air gap. The established signal gain is too large for the target's rotational magnetic signal at the given air gap.

Position 5. Running Mode Calibration corrects the signal gain to an optimal level for the installation air gap.

### Power Derating

The device must be operated below the maximum junction temperature of the device,  $T_{J(max)}$ . Under certain combinations of peak conditions, reliable operation may require derating supplied power or improving the heat dissipation properties of the application. This section presents a procedure for correlating factors affecting operating  $T_J$ . (Thermal data is also available on the Allegro MicroSystems Web site.)

The Package Thermal Resistance,  $R_{\theta JA}$ , is a figure of merit summarizing the ability of the application and the device to dissipate heat from the junction (die), through all paths to the ambient air. Its primary component is the Effective Thermal Conductivity,  $K$ , of the printed circuit board, including adjacent devices and traces. Radiation from the die through the device case,  $R_{\theta JC}$ , is relatively small component of  $R_{\theta JA}$ . Ambient air temperature,  $T_A$ , and air motion are significant external factors, damped by overmolding.

The effect of varying power levels (Power Dissipation,  $P_D$ ), can be estimated. The following formulas represent the fundamental relationships used to estimate  $T_J$ , at  $P_D$ .

$$P_D = V_{IN} \times I_{IN} \quad (1)$$

$$\Delta T = P_D \times R_{\theta JA} \quad (2)$$

$$T_J = T_A + \Delta T \quad (3)$$

For example, given common conditions such as:  $T_A = 25^\circ\text{C}$ ,  $V_{CC} = 12\text{ V}$ ,  $I_{CC} = 4\text{ mA}$ , and  $R_{\theta JA} = 140\text{ }^\circ\text{C/W}$ , then:

$$P_D = V_{CC} \times I_{CC} = 12\text{ V} \times 4\text{ mA} = 48\text{ mW}$$

$$\Delta T = P_D \times R_{\theta JA} = 48\text{ mW} \times 140\text{ }^\circ\text{C/W} = 7^\circ\text{C}$$

$$T_J = T_A + \Delta T = 25^\circ\text{C} + 7^\circ\text{C} = 32^\circ\text{C}$$

A worst-case estimate,  $P_{D(max)}$ , represents the maximum allowable power level ( $V_{CC(max)}$ ,  $I_{CC(max)}$ ), without exceeding  $T_{J(max)}$ , at a selected  $R_{\theta JA}$  and  $T_A$ .

*Example:* Reliability for  $V_{CC}$  at  $T_A = 150^\circ\text{C}$ , package SH (I1 trim), using minimum-K PCB

Observe the worst-case ratings for the device, specifically:  $R_{\theta JA} = 126^\circ\text{C/W}$ ,  $T_{J(max)} = 165^\circ\text{C}$ ,  $V_{CC(max)} = 24\text{ V}$ , and  $I_{CC(max)} = 16\text{ mA}$ .

Calculate the maximum allowable power level,  $P_{D(max)}$ . First, invert equation 3:

$$\Delta T_{max} = T_{J(max)} - T_A = 165^\circ\text{C} - 150^\circ\text{C} = 15^\circ\text{C}$$

This provides the allowable increase to  $T_J$  resulting from internal power dissipation. Then, invert equation 2:

$$P_{D(max)} = \Delta T_{max} \div R_{\theta JA} = 15^\circ\text{C} \div 126\text{ }^\circ\text{C/W} = 119\text{ mW}$$

Finally, invert equation 1 with respect to voltage:

$$V_{CC(est)} = P_{D(max)} \div I_{CC(max)} = 119\text{ mW} \div 16\text{ mA} = 7\text{ V}$$

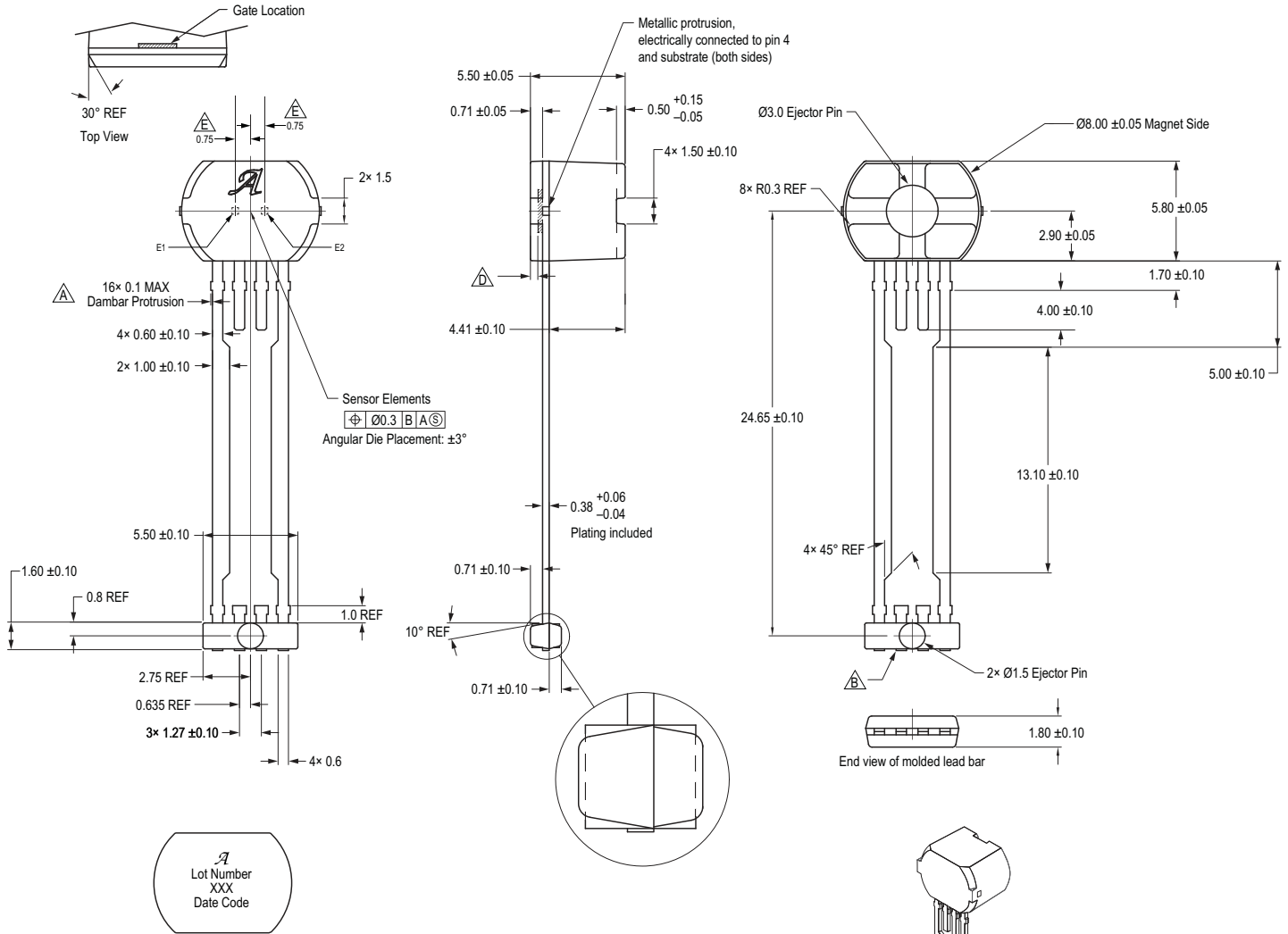
The result indicates that, at  $T_A$ , the application and device can dissipate adequate amounts of heat at voltages  $\leq V_{CC(est)}$ .

Compare  $V_{CC(est)}$  to  $V_{CC(max)}$ . If  $V_{CC(est)} \leq V_{CC(max)}$ , then reliable operation between  $V_{CC(est)}$  and  $V_{CC(max)}$  requires enhanced  $R_{\theta JA}$ . If  $V_{CC(est)} \geq V_{CC(max)}$ , then operation between  $V_{CC(est)}$  and  $V_{CC(max)}$  is reliable under these conditions.

## PACKAGE OUTLINE DRAWING

### For Reference Only – Not for Tooling Use

(Reference DWG-0000393)  
 Dimensions in millimeters. NOT TO SCALE.  
 Dimensions exclusive of mold flash, gate burrs, and dambar protrusions  
 Exact case and lead configuration at supplier discretion within limits shown



#### Standard Branding Reference View

Lines 1, 2, 3 = 7 characters.  
 Logo A molded in  
 Line 1: 7 digit alpha numeric Lot Number  
 Line 2: Last 3 digit of Part Number.  
 Additional suffixes may be added to Part number as required.  
 Line 3: 4 digit Date Code  
 Center align

- $\triangle$  Dambar removal protrusion (16x)
- $\triangle$  Molded Lead Bar for alignment during shipment
- $\triangle$  Branding scale and appearance at supplier discretion
- $\triangle$  Active Area Depth  $0.43 \pm 0.025$  mm
- $\triangle$  Hall elements (E1, E2); not to scale

### Package SH, 4-Pin SIP



### Revision History

Number	Date	Description
2	May 21, 2020	Minor editorial updates
3	June 17, 2021	Updated Package Outline Drawing (page 15)
4	October 1, 2022	Changed product status: Not for new design

Copyright 2022, Allegro MicroSystems.

Allegro MicroSystems reserves the right to make, from time to time, such departures from the detail specifications as may be required to permit improvements in the performance, reliability, or manufacturability of its products. Before placing an order, the user is cautioned to verify that the information being relied upon is current.

Allegro's products are not to be used in any devices or systems, including but not limited to life support devices or systems, in which a failure of Allegro's product can reasonably be expected to cause bodily harm.

The information included herein is believed to be accurate and reliable. However, Allegro MicroSystems assumes no responsibility for its use; nor for any infringement of patents or other rights of third parties which may result from its use.

Copies of this document are considered uncontrolled documents.

For the latest version of this document, visit our website:

[www.allegromicro.com](http://www.allegromicro.com)